Oil Shale, 2025, Vol. 42, No. 2, pp. 181–207
doi: https://doi.org/10.3176/oil.2025.2.03 ISSN 0208-189X

Mechanical properties and wellbore stability of the oil shale formation in the Shahejie Formation

Shuang Du[(a)], Houbin Liu[(a)]*, Shuai Wang[(a)],Shuai Cui[(b)], Jingyang Xi[(c)]

(a) State Key Laboratory of Oil and Gas Reservoir Geology and Exploitation, Southwest Petroleum University, 8 Xindu Avenue, Xindu District, Chengdu 610500, China
(b) Shale Gas Research Institute, PetroChina Southwest Oil & Gasfield Company, 5 Section 1, Fuqing Road, Chengdu 610051, China
(c) Sinopec Shengli Petroleum Engineering Co., Ltd., 258 Jinan Road, Dongying, Shandong 257100, China

Received 25 October 2024, accepted 9 April 2025, available online 11 April 2025

Abstract. *Significant progress has been made in the exploration and development of oil shale in Sinopec's K-II block. However, frequent downhole blockages, drilling incidents, and wellbore instability have posed challenges for high-inclination horizontal drilling. This study analyzes complex subsurface conditions using field data and core experiments to investigate the physical, chemical, and mechanical properties of the formation. Key factors driving oil shale collapse are identified, and a wellbore stability evaluation method for the Shahejie Formation is developed. Results show that the formation has well-developed fractures, with quartz and clay as its primary components, and that water-based drilling fluids have minimal impact on its mechanical properties. Wellbore stability is significantly affected by inclination, azimuth, and weak-plane fractures. The critical collapse pressure equivalent density ranges from 1.5 to 1.65 g/cm³. Drilling along the maximum horizontal stress improves stability compared to drilling along the minimum stress. Enhancing drilling fluid sealing and adding rigid particles further improve wellbore integrity. These findings provide practical insights for safer oil shale drilling operations.*

Keywords: *critical collapse pressure equivalent density, drilling directions, fracture, oil shale, wellbore stability.*

1. Introduction

During oil and gas exploration and development, wellbore stability is the main factor restricting drilling speed, a challenge that is particularly prominent in

* Corresponding author, 1005839481@qq.com

shale formations. Domestic and international statistical data show that >90% of well collapses occur in shale formations, with hard and brittle shale formations accounting for 65% [1, 2]. Many experts have conducted considerable research on the problem of wellbore instability in shale formations.

The mechanical approaches to wellbore stability began with Westergaard's study in 1940 [3]. Subsequent researchers refined the purely mechanical methods and investigated wellbore stability from various perspectives, including principal stress directions [4], borehole and bedding orientations [5, 6], rock anisotropy [7–10], fluid flow and poroelasticity [11, 12], and failure criteria [13, 14].

In recent years, scholars have conducted more comprehensive and in-depth research on shale wellbore stability, focusing on aspects such as drilling fluid properties, the macro- and microstructure of rocks, complex constitutive relationships, high-temperature properties of oil shale, and multiphysics coupling.

Zhu et al. [15] analyzed the causes of wellbore collapse in the Nanpu No. 3 structure from the aspects of physical and chemical properties of shale, macro- and microstructure, mechanical properties, rock mechanics, and the chemical coupling of the drilling fluid. Their work effectively solved the problem of wellbore stability in shale formations. A set of drilling fluid technologies suitable for the deep brittle mud shale in the Nanpu No. 3 structure was developed.

Liang et al. [16] quantitatively analyzed the effects of drilling fluid on weak surface strength, matrix strength, and pore space in rocks. A coupled seepage and wellbore stability model was established based on linear elastic theory and a single weak-surface criterion, incorporating weak surface structure, hydration, and seepage. The results indicated that weak surface structure significantly affects collapse pressure, with its changes influencing pressure distribution. In contrast, seepage stress has minimal impact on collapse pressure during the initial drilling stage but becomes prominent in the later stages.

Qian et al. [17] developed an all-oil-based drilling fluid system with a temperature resistance of 150 °C and a density of 1.55 g/cm^3. Their system offers excellent comprehensive performance, including good rheology, inhibition, plugging, pollution resistance, lubricity, and high-temperature stability, effectively controlling the hydration expansion of oil shale and solving the problem of wellbore instability in oil shale formations.

Liu et al. [18] established a stress distribution model for the borehole under mechanical-chemical coupling, calculated the borehole wall collapse pressure using failure criteria, and obtained a reasonable anti-collapsing drilling fluid density.

Chen et al. [19] determined the distribution of microfractures in hard and brittle mud shale using a random function, and established a damage constitutive model by combining damage and fracture mechanics. FLAC3D software was used to analyze the effects of drilling fluid, microfracture morphology, and other factors on mud shale failure. The results showed that drilling fluid and the development degree of microfractures have the greatest impact on wellbore stability, while the direction of microfractures has the least influence.

Zhao et al. [20] studied the relation between longitudinal wave velocity, peak strength, and the elastic modulus of oil shale and temperature, establishing a micro-unit thermal damage constitutive model. They found that when the temperature exceeded the threshold value, the main driving force behind the increasing thermal damage during the pyrolysis of organic matter and the rapid increase in thermal damage differed significantly from that observed below the temperature threshold. This difference is clearly reflected in physical and mechanical properties, damage factors, microstructure, and the determined model parameters.

Zhao et al. [21] studied the permeability of oil shale at different temperatures using a triaxial permeability testing machine. The results showed that oil shale is nearly impervious between 20 and 350 °C. At 350 °C, permeability initially increases due to ambient and additional expansion stresses, but then decreases to near zero. From 350 to 600 °C, permeability increases sharply, peaking at 600 °C. The threshold temperature for permeability change is 350 °C, and permeability decreases as pore pressure increases at various temperatures.

Zhang et al. [22] built a calculation model for shear stress and normal stress on any fracture surface occurrence based on shale formation fracture surface occurrence, developed a multifield coupling model of laminar flow, and solidified hot wall stability with a fracture surface. This model is based on the failure criterion that shear stress on the fracture surface exceeds the friction force. Formation fractures and seepage will increase formation collapse pressure to varying degrees, while low-temperature and low-activity drilling fluid can effectively reduce wellbore collapse pressure.

Ren et al. [23] studied the impact of oil shale's shear characteristics at real-time high temperature on the stability of injection and production wells and oil and gas production. Their results showed that the shear strength and shear modulus of oil shale at real-time high temperatures decreased with increasing shear angle. They found that with rising temperature, shear strength and shear modulus first decrease and then increase, reaching a minimum value at 400 °C. During this process, the energy accumulated in the elastic and crack propagation stages is released, with a large amount of energy discharged during instability failure. Meanwhile, the failure mode of oil shale changes from brittle to ductile, and secondary cracks gradually increase, with failure characteristics changing from a through type to a non-through type.

Wang et al. [24] designed an experimental device for oil shale pyrolysis using steam injection in a large reactor and studied its pore-fracture structure. Their results revealed that during high-temperature steam pyrolysis, numerous microfractures formed in the oil shale, along with obvious fracturing of the rock bedding surface, which could provide good channels for steam injection and oil and gas flow.

Feng et al. [25] used a high-temperature, high-pressure triaxial testing machine and stress micro-CT technology to explore the evolution of oil shale permeability, pyrolysis gas production, mesostructure, and axial deformation with temperature (≥300 °C). The results showed that there is a threshold temperature for the evolution of oil shale permeability. Under fixed stress conditions (axial pressure of 10 MPa, confining pressure of 7 MPa), this threshold temperature is 400 °C. When the pyrolysis temperature is below the threshold, permeability is greatly affected by rock strength and is negatively correlated with temperature. When the pyrolysis temperature exceeds the threshold, permeability is dominated by the degree of pyrolysis and becomes positively correlated with temperature.

Zhang et al. [26] explored the anisotropic heat transfer characteristics of oil shale in laboratory experiments, and the experimental results showed that the thermal conductivity of oil shale bedding decreased with the increase of temperature, but conductivity is higher in the direction parallel to the bedding plane than in the direction vertical to it. Specific heat capacity is greatly affected by temperature, decreasing as temperature rises, and reaching its maximum at 400 °C. By observing the micro-CT image, it was found that the increase of fractures is highly sensitive to heat conduction in the direction of vertical bedding.

Cao et al. [27] used a steam generator to study the shear characteristics of oil shale at different temperatures and shear angles. Their results showed that temperature significantly affects the failure characteristics of oil shale. Brittle failure characteristics were obvious at temperatures below 300 °C, while ductile failure characteristics became more apparent at 400 and 500 °C. The cohesion of oil shale first increases and then decreases with rising temperature, whereas the change of internal friction angle follows the opposite trend. Shear strength decreases with the increase of shear angle. With higher steam temperatures, the shear failure mode of oil shale shows more complex failure characteristics.

Currently, the literature has not yet established a comprehensive evaluation method for wellbore stability in the Shahejie Formation. To devise an effective solution to the problem of borehole collapse in this formation, we first analyzed the mineral composition, microstructural characteristics, and mechanical properties of the rock in the collapsed zones through a series of laboratory experiments, and determined the main factors leading to wellbore instability. Based on these controlling factors and laboratory data, we conducted a detailed assessment of how key factors, such as borehole trajectory changes, the mechanical weak-surface effect of fractures, and bottom-hole pressure penetration, affect formation wall stability. Our analysis revealed the complex interactions between each factor and wellbore stability. Finally, based on the above research, we established a set of evaluation and prediction methods for the wellbore stability of the Shahejie Formation. These research results provide scientific and technical support for safe drilling of oil shale in the

Shahejie Formation, enhancing our understanding of the complex mechanical behavior of oil shale formations and providing important guidance for practical drilling engineering.

2. Materials and methods

2.1. Mineral composition of oil shale

Using oil shale samples from different well depths in the Shahejie Formation as the research object, an X-ray diffractometer was used to test and analyze their mineral composition, as shown in Figure 1. The XRD pattern is presented in Figure 2.

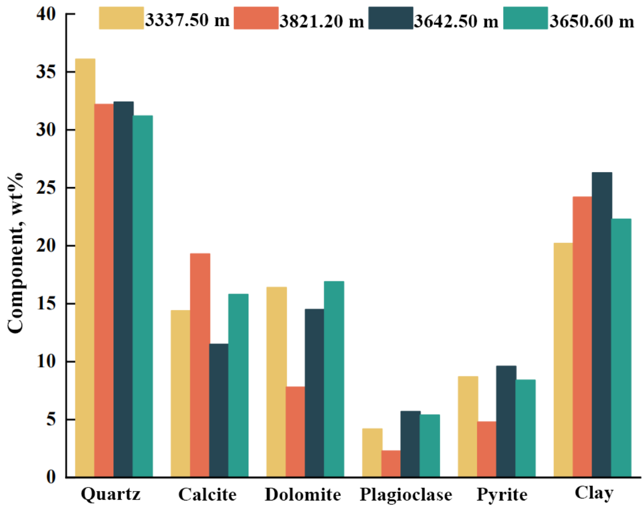

Fig. 1. Mineral composition distribution of Shahejie Formation oil shale.

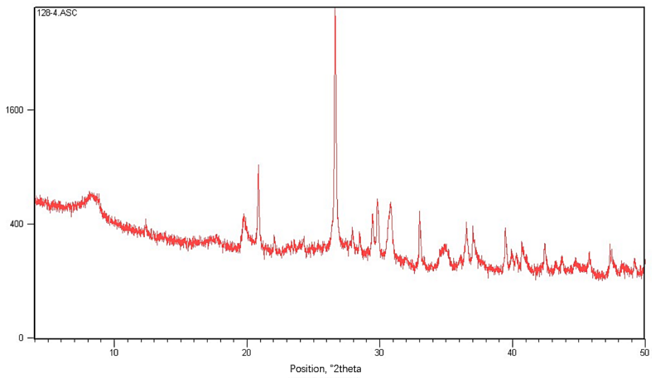

3337.50 m

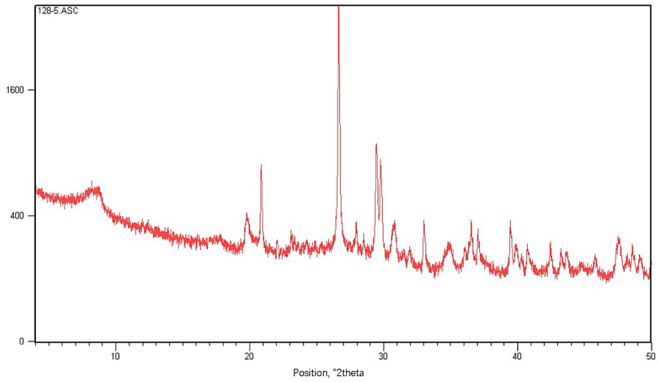

3821.20 m

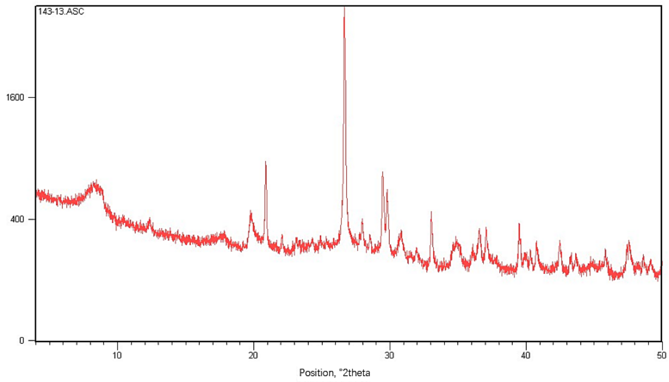

3642.50 m

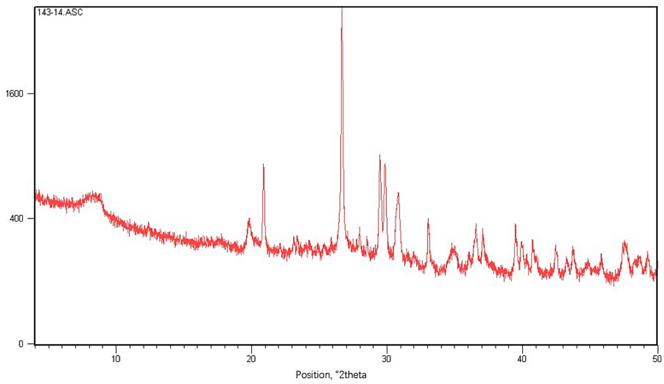

3650.60 m

Fig. 2. XRD patterns at different well depths.

The mineral composition of Shahejie Formation oil shale is mainly quartz and clay, with quartz generally accounting for >30% of the content and clay minerals for >22%. In addition, small amounts of calcite, dolomite, plagioclase, and other minerals were identified. The clay minerals in this formation are mainly non-expansive, resulting in relatively weak hydration expansion capacity.

2.2. Oil shale material

The microstructure of oil shale was analyzed using scanning electron microscopy, and the results are shown in Figure 3.

As can be seen from Figure 3, the Shahejie Formation oil shale rock body exhibits a relatively dense structure. However, due to its hardness and brittleness, microfractures easily form under high stress or external loads. These microcracks run throughout the entire field of view, with crack widths of ~2–3 μm. The dissolution cavities are relatively well-developed, which may further affect the permeability and strength of the rock.

To better understand the spatial distribution characteristics of oil shale fractures, CT scanning was used to examine two sets of cube rock samples with a side length of 5 cm. The scans were processed using Avizo, a specialized three-dimensional visualization software, which revealed the shape and orientation of the fractures, as shown in Figure 4.

Comparing and analyzing the oil shale CT images of the Shahejie Formation reveals that the two groups of oil shale rock bodies exhibit multiple types of fractures. The first type comprises lithologic interfacial fractures and closed fractures. Lithologic interfacial cracks occur along the contact surfaces between different rock types or lithologies. These interfaces often exist between rock layers with varying mechanical properties, such as elastic modulus and tensile strength. Differential deformation or stress concentrations at these

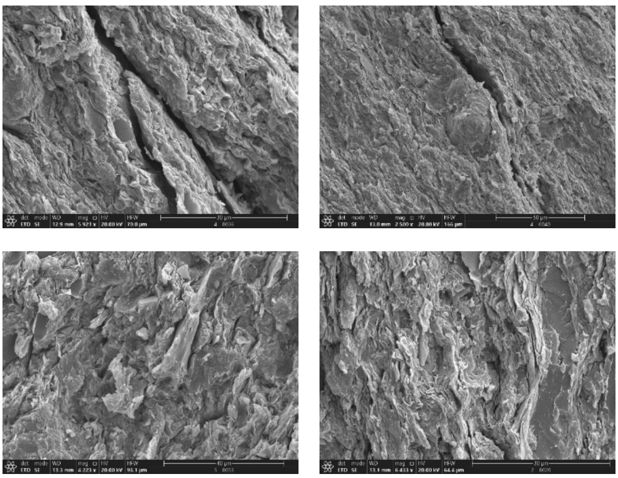

Fig. 3. Scanning electron microscopy images of Shahejie Formation oil shale.

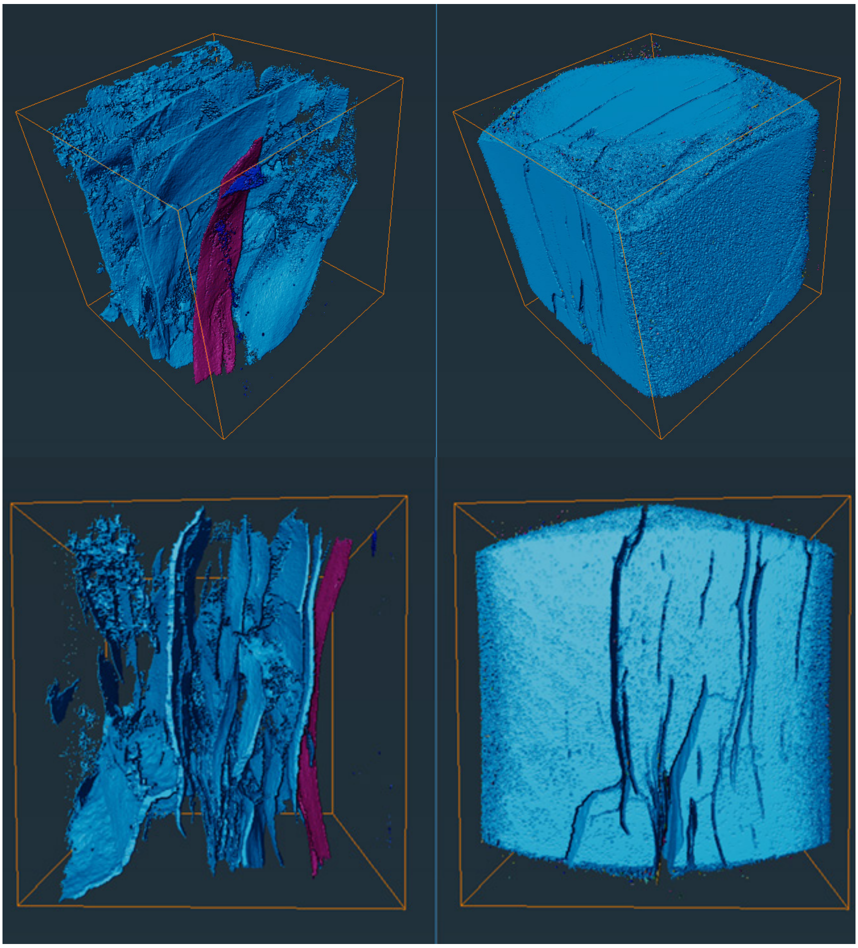

Fig. 4. CT images of Shahejie Formation oil shale.

interfaces under geological stress conditions can lead to the initiation and propagation of cracks along the interfaces. Closed fractures, on the other hand, are fractures where the crack surfaces are in contact without significant openings. They typically form due to early geological processes, such as tectonic movements or diagenesis. Over time, these cracks can close due to compaction, pressure from overlying strata, or mineral precipitation. Despite being closed, they may still represent planes of weakness within the rock mass. The other type of fracture comprises induced cracks and open cracks. Induced cracks are caused by external mechanical factors, such as changes in ground stress and osmotic pressure, reflecting the mechanical characteristics of the rock mass under specific geological and engineering conditions. Open cracks form under tensile stress and are not filled with other minerals, reflecting the failure of the rock mass under specific stress conditions.

2.3. Experiments

To further explore the mechanism of wellbore instability in oil shale formations, a set of wellbore stability evaluation models was established based on laboratory test data of rock mechanics and basic physical property parameters.

First, the permeability parameters and transverse wave velocity of oil shale samples with different fracture development characteristics were measured. The porosity and permeability of the oil shale were determined using an automatic gas porosity-permeability meter, allowing for the quantitative evaluation of the rock wall's seepage characteristics. These experimental data can be used to further study the dynamic variations in the wellbore-formation stress field and seepage field [17]. In addition, the acoustic velocity of the oil shale was obtained using the pulse transmission method.

Second, the mechanical properties of the oil shale were analyzed in detail. A series of systematic triaxial mechanics experiments were conducted using a triaxial mechanical testing machine in both static and dynamic states. This equipment can simulate the actual underground mechanical environment to accurately obtain the key mechanical characteristics of the oil shale. Through these experiments, we gained a deeper understanding of the influence of different fracture development characteristics and drilling fluid systems on the mechanical properties of oil shale, so as to establish a more accurate prediction model of oil shale wellbore stability [18, 19].

Finally, the shear strength of the oil shale, along with the cohesion and internal friction angle of the shear failure surface, was obtained through direct shear tests, further improving the comprehensive evaluation of rock mechanical properties.

2.3.1. Experimental test of physical properties of rock foundation

The porosity, permeability, and acoustic velocity of the oil shale were obtained using a rock porosity-permeability tester and an acoustic wave tester, as shown in Figure 5 below.

The oil shale rock of the Shahejie Formation is highly dense, with porosity ranging from 0.25% to 0.49% and permeability ranging from 4.58×10^{-4} to 2.39×10^{-3} mD. The P-wave and S-wave velocities are in the ranges of 2241–2613 and 1310–1606 m/s, respectively, reflecting the elastic response of the rock mass. The microfractures in the oil shale are relatively well-developed, and the differences in petrophysical parameters are closely related to the development of these fractures. The existence and distribution of fractures enhance the anisotropy of the rock, which affects its porosity parameters and acoustic velocity. As seepage channels, fractures can induce drilling fluid invasion into the formation, causing wellbore instability [20].

To further understand the variation in rock porosity and permeability of the borehole wall in different well-inclined sections, experimental tests were carried out on downhole cores with varying bedding angles (0°, 30°, 45°, 60° and 90°). The experimental data are shown in Table 1.

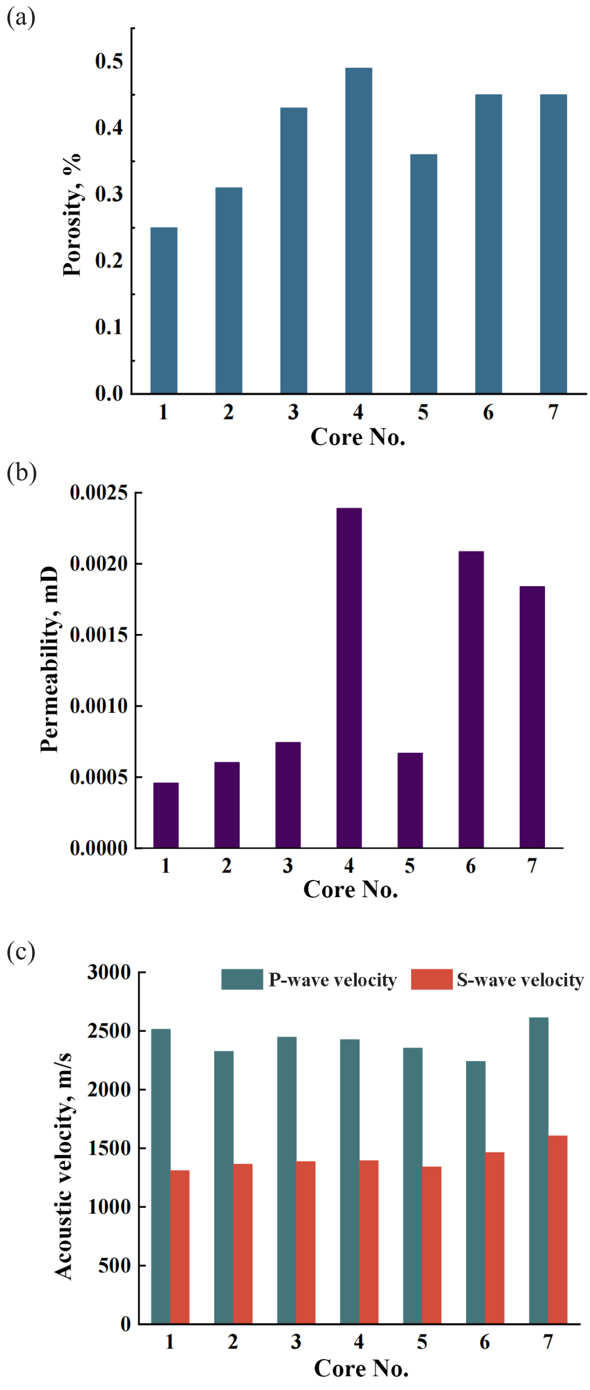

Fig. 5. Core porosity (a), permeability (b), and acoustic velocity (c) test results.

Table 1. Anisotropy test results of porosity and permeability of oil shale

Bedding angle, °	Length, cm	Diameter, cm	Porosity, %	Permeability, mD	Average porosity, %	Average permeability, mD
0	5.016	2.468	0.25	4.32×10^{-4}	0.28	4.69×10^{-4}
0	5.030	2.492	0.31	5.06×10^{-4}		
30	4.738	2.500	0.43	5.98×10^{-4}	0.46	5.30×10^{-4}
30	4.492	2.476	0.49	4.61×10^{-4}		
45	5.030	2.492	0.41	6.68×10^{-4}	0.53	6.47×10^{-4}
45	4.990	2.512	0.64	6.26×10^{-4}		
60	5.018	2.518	0.99	1.21×10^{-3}	0.72	1.38×10^{-3}
60	5.036	2.502	0.45	1.54×10^{-3}		
90	4.430	2.514	1.98	1.663×10^{-3}	1.97	1.63×10^{-3}
90	4.432	2.492	1.95	1.602×10^{-3}		

As shown in Table 1, the anisotropy characteristics of rock porosity and permeability in the borehole wall across different well-inclined sections are obvious. The porosity and permeability of the rock (bedding angle 0°) in the vertical well section are low, with an average porosity of 0.28% and an average permeability of 4.69×10^{-4} mD. As the inclination angle increases, the porosity and permeability of the borehole rock show an upward trend, reaching their maximum in the horizontal section (bedding angle 90°), with an average porosity of 1.97% and permeability of 1.63×10^{-3} mD. In general, the oil shale strata in the K-II block are relatively compact, with low porosity and permeability.

2.3.2. Experimental test of rock mechanical properties

The mechanical parameters of oil shale were determined experimentally, and the effects of fractures and drilling fluid on its mechanical properties were analyzed, as shown in Table 2. To approximate in situ conditions as closely as possible, the confining pressure for the experiment was estimated based on the depth of the cored formation.

The overall mechanical strength of the oil shale is low. The maximum compressive strength under an underground mechanical environment is 183.5 MPa, while the minimum compressive strength is only 37.2 MPa. In terms of rock failure, the oil shale rock mass exhibits a variety of failure modes, mainly tensile failure and simple shear failure. When the confining pressure is low, the rock is dominated by tensile fracture failure. As the

Table 2. Experimental results for triaxial mechanics of oil shale

Sample No.	Experiment condition	Confining pressure, MPa	Compressive strength, MPa	Elastic modulus, MPa	Poisson's ratio	Core description
1	Dry sample	30	183.5	19,310.90	0.170	Homogeneous sample
2			62.5	9,678.95	0.150	Filling fracture development
3			46.8	6,958.32	0.127	No filling fracture development
4	Drilling fluid immersion	30	176.4	18,425.58	0.168	Homogeneous sample
5			52.3	9,236.54	0.146	Filling fracture development
6			37.2	6,287.6	0.120	No filling fracture development

confining pressure increases, the connectivity of the rock mass improves, leading to shear failure as the failure mode, with the oil shale exhibiting more complex deformation and failure mechanisms.

The data in Table 1 reflect the differences in mechanical properties between non-fractured oil shale and fractured rock, both filled and unfilled. Specifically, the mechanical properties of non-fractured oil shale are the highest. Fractures have a great impact on the mechanical properties of oil shale. When cracks are filled and closed, the strength of the oil shale is slightly improved, but still lower than that of oil shale without cracks. This indicates that the connectivity and consistency of the rock mass are enhanced by filling, but the mechanical properties of the non-fractured state cannot be completely restored. Due to the non-expansive nature of the oil shale's clay minerals, drilling fluid immersion has little effect on the mechanical properties of the rock.

Observations of rock samples after triaxial mechanical testing reveal that whether the fracture is unfilled or filled, oil shale tends to fail along the fracture direction when subjected to external stress. This phenomenon further confirms the priority of fracture failure in a high external stress environment. A comparative analysis of the experimental data indicates that hydration has little effect on the mechanical characteristics and wellbore stability of oil shale. Fractures are relatively developed in oil shale, and the existence of weak surfaces in oil shale's mechanics is the main factor affecting wellbore stability.

2.3.3. Direct shear test

The direct shear test of oil shale was performed using a rock direct shear instrument. The photos and data of the experiment are shown in Figure 6.

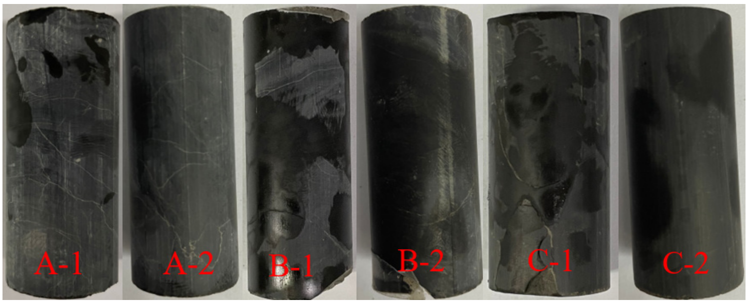

Rock samples before the direct shear test

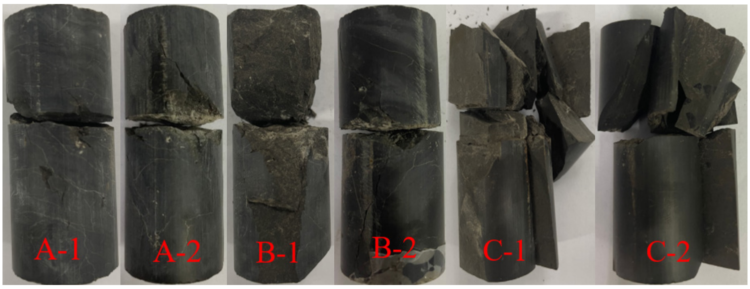

Rock samples after the direct shear test

Fig. 6. Photographs of rock samples before and after the direct shear test.

Table 3. Results of the direct shear test

Sample No.	Positive stress, MPa	Peak shear stress, MPa	Internal friction angle, °	Cohesion, MPa
A-1	0	3.918	23.85	3.918
A-2	5	6.128		
B-1	0	11.230	31.70	11.230
B-2	5	14.318		
C-1	0	6.052	45.79	6.052
C-2	5	11.192		

A comparative analysis of the experimental results indicates that oil shale with developed fractures exhibits low shear strength. The cohesion of the rock is generally 3.918–11.230 MPa, while the internal friction angle falls between 23.85–45.79°. These parameters reflect the resistance and deformation characteristics of the rock under shear stress. The existence of cracks provides an easier path for rock shear slip, which promotes the occurrence of wellbore instability.

2.4. Calculations

2.4.1. Theoretical model of the well circumferential stress field

Compared to vertical wells, highly inclined and horizontal wells exhibit significantly different wellbore stability, influenced not only by the drilling trajectory but also by the orientation of the in situ stresses. Therefore, the study of borehole mechanical stability for highly deviated wells and horizontal wells should start from understanding the stress field around the well, selecting appropriate mechanical strength criteria, and establishing a reasonable prediction model to determine the safe drilling fluid density for deviated and horizontal wells.

The presence of a borehole alters the distribution of the original in situ stress field. To accurately assess the stresses around the wellbore, stress analysis must be conducted in the borehole coordinate system. Transforming the in situ stresses from the ground coordinate system to the borehole coordinate system ensures that the calculated stress components directly correspond to the actual stress conditions experienced by the wellbore.

By combining the inclination and azimuth of the borehole trajectory with the stress field in the Cartesian coordinate system, the stress field relative to the borehole axis for any azimuth and inclination can be obtained using the Cartesian coordinate transformation. The transformation equation is as follows [28]:

$$\begin{aligned}
\sigma_x &= \cos^2\alpha\left(\sigma_H\cos^2\beta+\sigma_h\sin^2\beta\right)+\sigma_h\sin^2\beta \\
\sigma_y &= \sigma_H\sin^2\beta+\sigma_h\cos^2\beta \\
\sigma_z &= \sin^2\alpha\left(\sigma_H\cos^2\beta+\sigma_h\sin^2\beta\right)+\sigma_v\cos^2\alpha \\
\tau_{xy} &= \cos\alpha\sin\beta\cos\beta\left(\sigma_h-\sigma_H\right) \\
\tau_{xz} &= \cos\alpha\sin\alpha\left(\sigma_H\cos^2\beta+\sigma_h\sin^2\beta-\sigma_v\right) \\
\tau_{yz} &= \sin\alpha\cos\beta\sin\beta\left(\sigma_h-\sigma_H\right)
\end{aligned}, \tag{1}$$

where σ_H is the maximum horizontal principal stress (MPa), σ_h is the minimum horizontal principal stress (MPa), α is the inclination of the borehole trajectory (°), β is the azimuth angle of the wellbore trajectory (°), and σ_v is the vertical principal stress (MPa). In the column coordinate system, the effective stress field ($r = r_w$) of the surface of an arbitrarily inclined shaft wall can be expressed as follows:

$$\begin{aligned}
&\sigma_r = P_w - ap(r,t) \\
&\sigma_\theta = (\sigma_x + \sigma_y) - P_w - (\sigma_x - \sigma_y)\cos 2\theta - 4\times\tau_{xy}\times\sin 2\theta - ap(r,t) \\
&\sigma_{zz} = \sigma_z - \mu\left[2(\sigma_x - \sigma_y)\cos 2\theta + 4\tau_{xy}\sin 2\theta\right] - ap(r,t) \\
&\tau_{\theta z} = 2(-\tau_{xz}\sin\theta + \tau_{yz}\cos\theta) \\
&\tau_{r\theta} = \tau_{rz} = 0
\end{aligned}, \quad (2)$$

where σ_x, σ_y, σ_z, τ_{xy}, τ_{xz}, and τ_{yz} are the ground stress components (MPa), σ_r, σ_θ, σ_{zz}, $\tau_{\theta z}$, and $\tau_{r\theta}$ are the stress components in cylindrical coordinates (in MPa), P_w is the liquid column pressure (MPa), θ is the well circumference angle (°), μ is Poisson's ratio (dimensionless), a is the effective stress coefficient (dimensionless), $p(r,t)$ is the formation pore pressure (MPa), whose distance from the well wall is r, and t is time.

2.4.2 Theoretical model of weak surface fractures

The existence of weak surfaces can change the physical characteristics of oil shale and the stress distribution around the well. Given that fractures are relatively common in oil shale formations, the influence of weak surfaces on wellbore stability can be analyzed using a mechanical weak-surface criterion. The theoretical model is shown below [29]:

$$\sigma_1 = \sigma_3 + \frac{2(C_w + \sigma_3\tan\varphi_w)}{(1-\tan\varphi_w\cot\delta)\sin 2\delta} \quad (\delta_1 \le \delta \le \delta_2), \quad (3)$$

$$\begin{cases}
\delta_1 = \dfrac{\varphi_w}{2} + \dfrac{1}{2}\arcsin\left[\dfrac{(\sigma_1 + \sigma_3 + 2C_w\cot\varphi_w)\sin\varphi_w}{\sigma_1 - \sigma_3}\right] \\
\delta_2 = \dfrac{\pi}{2} + \dfrac{\varphi_w}{2} - \dfrac{1}{2}\arcsin\left[\dfrac{(\sigma_1 + \sigma_3 + 2C_w\cot\varphi_w)\sin\varphi_w}{\sigma_1 - \sigma_3}\right]
\end{cases}, \quad (4)$$

where σ_1 is the maximum horizontal principal stress (MPa), σ_3 is the minimum horizontal principal stress (MPa), C_w is the weak surface cohesion (MPa), and φ_w is the weak surface friction angle (°). If the above conditions are not met, the rock failure follows the Mohr–Coulomb criterion:

$$\sigma_1 = \sigma_3\cot^2\left(\frac{\pi}{2} - \frac{\varphi_0}{2}\right) + 2C_0\cot\left(\frac{\pi}{2} - \frac{\varphi_0}{2}\right) \quad (\delta \ge \delta_2,\ \delta \le \delta_1), \quad (5)$$

where C_0 denotes rock cohesion (MPa), and φ_0 denotes the rock internal friction angle (°).

Collapse pressure can be calculated as follows:

$$P_t = \frac{\sigma_H + \sigma_h - 2(\sigma_H - \sigma_h)\cos 2\theta + \alpha P_p (K^2 - 1) - 2CK + \sigma'_\theta - \sigma'_r K^2}{K^2 + 1}, \quad (6)$$

$$\text{with } K = \cot\left(\frac{\pi}{4} - \frac{\varphi}{2}\right),$$

where C is rock cohesion (MPa), P_p is formation pore pressure (MPa), φ is the rock internal friction angle (°), σ'_θ is effective circumferential stress (MPa), σ'_r is effective radial stress (MPa), and α is the Biot coefficient, with the other symbols being the same as above.

2.4.2. Theoretical model of the wellbore-formation seepage field

Fractures in oil shale formations are relatively well-developed, and the seepage capacity of the borehole is influenced by the direction of fracture extension. The spatial relationship between the fractures and the borehole can be evaluated by analyzing their orientation and positioning. The theoretical model is shown below [30]:

$$K_R = K_{11}\sin^2\theta_1 + K_{33}\cos^2\theta_1 = \frac{K_{11} + K_{33}}{2} - \frac{K_{11} - K_{33}}{2}\cos 2\theta_1 , \quad (7)$$

where K_R is the radial seepage capacity of the shaft wall (d), K_{11} and K_{33} are the three-dimensional permeability components (d), and θ_1 is the angle between the bedding plane and the X axis (°).

Evaluating the anisotropy of wellbore permeability characteristics in oil shale formations requires determining the relationship between the radial seepage direction and the angle of the wellbore fracture surface at different positions of horizontal wells. To evaluate the anisotropy of wellbore seepage characteristics, the relationship between the radial seepage and the angle of the fracture surface should be established. The relationship between the radial seepage and the angle of the normal direction of the fracture surface can be expressed as follows [31]:

$$\xi = \arccos\left(\frac{a_1 \cdot b_1 + a_2 \cdot b_2 + a_3 \cdot b_3}{\sqrt{a_1^2 + a_2^2 + a_3^2} \cdot \sqrt{b_1^2 + b_2^2 + b_3^2}}\right) \cdot \frac{180}{\pi}, \quad (8)$$

with

$$a_1 = \sin\alpha_s \cos\beta_s$$
$$a_1 = \sin\alpha_s \sin\beta_s$$
$$a_3 = \cos\alpha_s$$
$$b_1 = \cos\alpha\cos\beta\cos\theta - \sin\alpha\sin\theta ,$$
$$b_2 = \sin\alpha\cos\beta\cos\theta + \cos\alpha\sin\theta$$
$$b_3 = -\sin\beta\cos\theta$$

where ξ is the angle between the radial flow direction and the fracture surface along the well wall (°), α_s and β_s are the fracture inclinations (°), α is the inclination angle of the well track (°), β is the azimuth angle of the wellbore trajectory (°), and θ is the angle around the well (°).

Combined with the test data of oil shale porosity and permeability, the influence of borehole trajectory changes on the porosity and permeability of the Shahejie Formation was calculated and analyzed using Mathcad software, as shown in Figure 7.

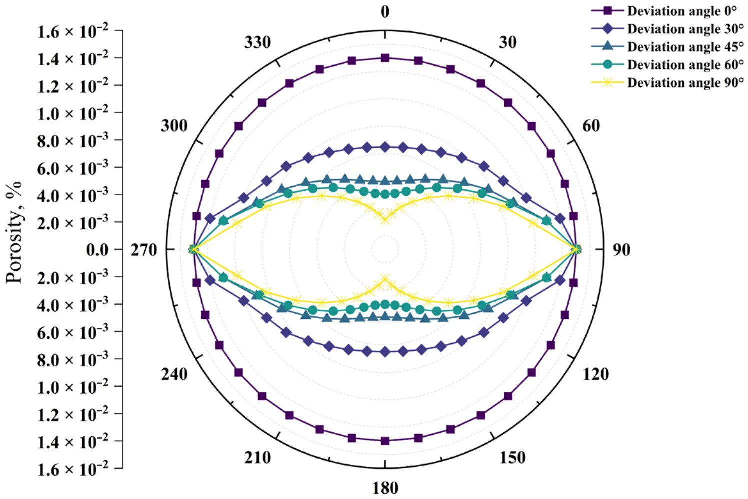

Effect of borehole trajectory on borehole porosity

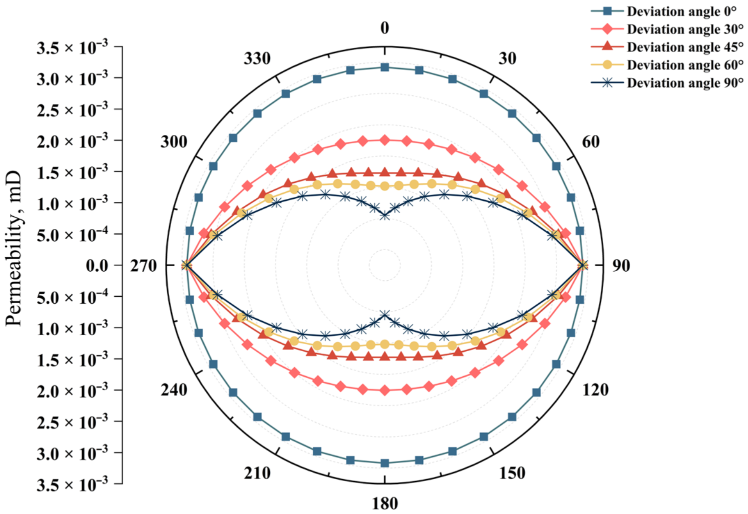

Effect of borehole trajectory on borehole permeability

Fig. 7. Distributions of wellbore porosity and permeability under different borehole paths.

A comparative analysis of Figure 7 shows that there are significant differences in the porosity and permeability of different inclined sections of the oil shale formation. The porosity and permeability parameters of the vertical section are relatively high. With the increase in the inclination angle, both the porosity and permeability gradually decrease.

2.4.3. Evaluation of wellbore stability in oil shale formations

According to on-site seismic data, the maximum horizontal in situ stress of the Shahejie Formation oil shale is 2.55 MPa/100m, the minimum horizontal in situ stress is 2.05 MPa/100m, and the overlying in situ stress is 2.5 MPa/100m. Based on the above theoretical model, the wellbore stability of the oil shale formation was evaluated and analyzed. The effects of different drilling directions, the mechanical weak surface effect of fractures, and drilling fluid pressure penetration effects on wellbore stability were predicted, as shown in Figures 8 and 9.

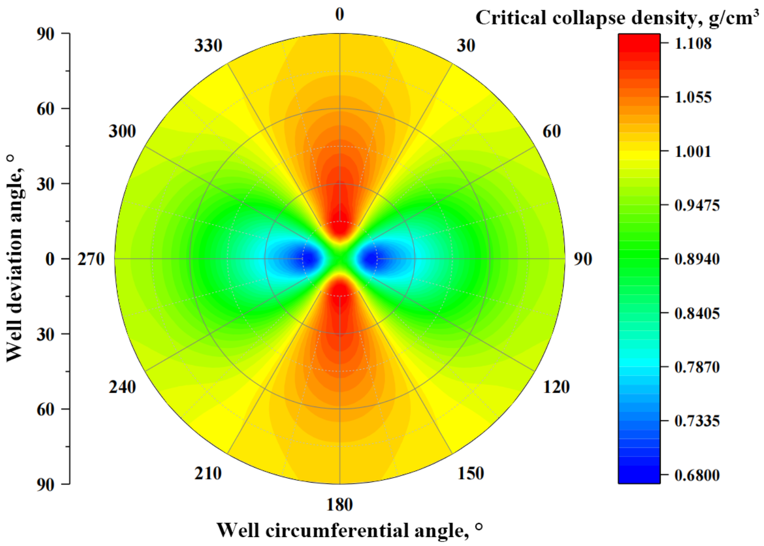

Influence of well circumference / inclination angle on collapse density
(without considering the weak surface effects of fracture mechanics)

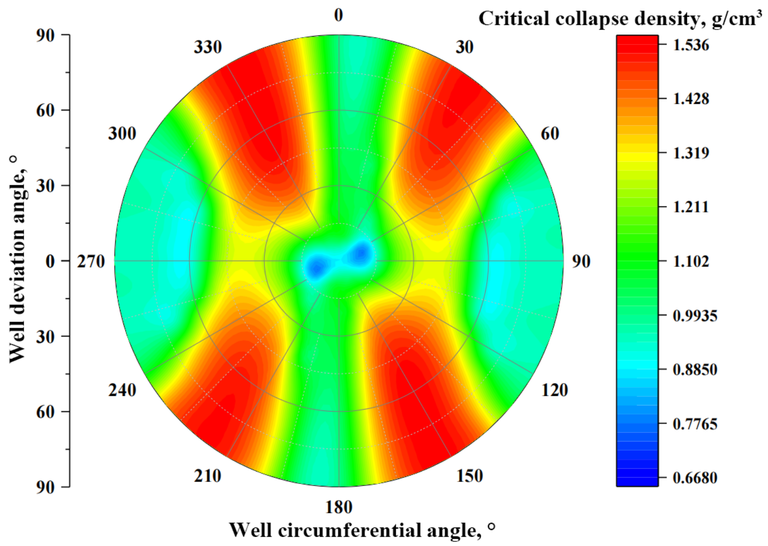

Influence of well circumference / inclination angle on collapse density
(considering the weak surface effects of fracture mechanics)

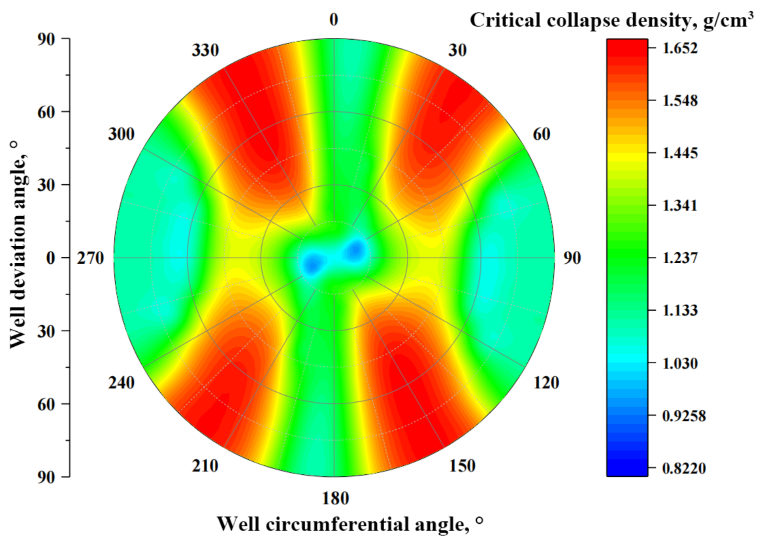

Influence of well circumference / inclination angle on collapse density
(considering the weak surface effects of fracture mechanics and pressure penetration)

Fig. 8. Drilling horizontal wells along the minimum horizontal principal stress.

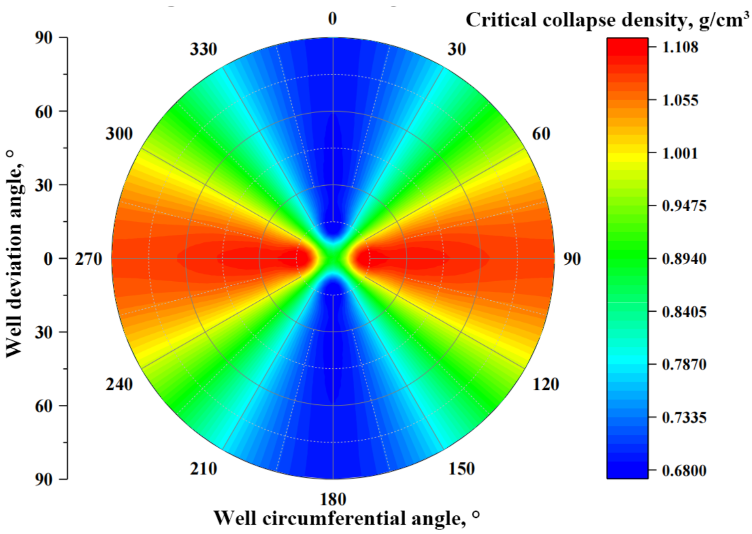

Influence of well circumference / inclination angle on collapse density (without considering the weak surface effects of fracture mechanics)

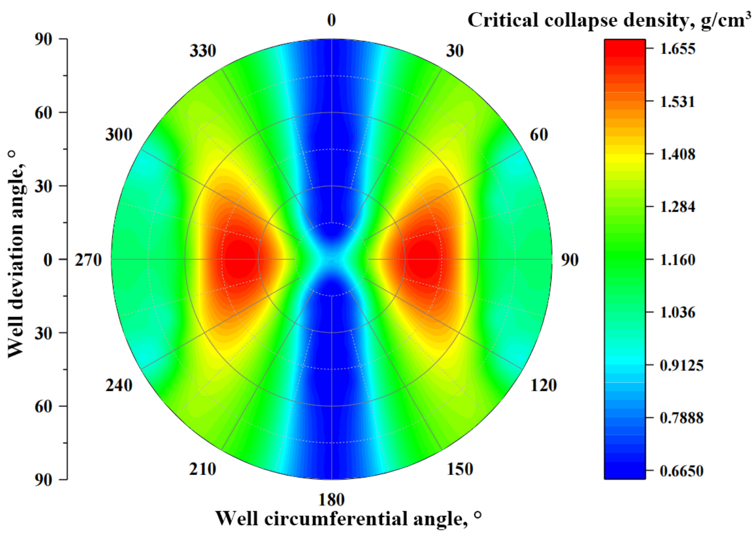

Influence of well circumference / inclination angle on collapse density (considering the weak surface effects of fracture mechanics)

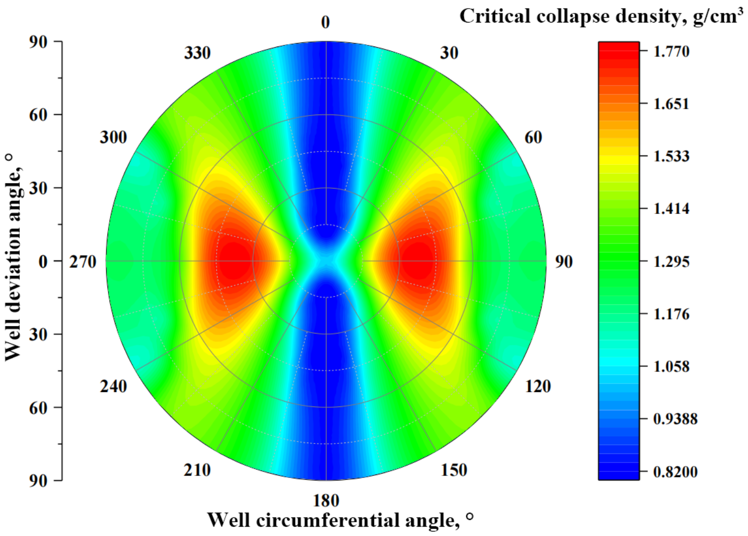

Influence of well circumference / inclination angle on collapse density
(considering the weak surface effects of fracture mechanics and pressure penetration)

Fig. 9. Drilling horizontal wells along the maximum horizontal principal stress.

It can be seen that different drilling directions have a significant impact on the wellbore stability of oil shale formations in the Shahejie Formation. In general, drilling horizontal wells along the direction of maximum horizontal principal stress results in better stability. For horizontal wells drilled along the minimum horizontal principal stress, the collapse pressure equivalent density in the well inclination angle range of 45–90° is generally >1.55 g/cm^3, which makes the borehole wall more prone to collapse and instability. In contrast, for horizontal wells drilled along the maximum horizontal principal stress, the area with high collapse pressure equivalent density is small, mainly concentrated in the well inclination angle range of 25–45°, where the wellbore stability is better.

3. Analysis and discussion

To verify the accuracy of the established evaluation method for wellbore stability, combined with the in situ downhole complexity and engineering information of two complex wells drilled in the Shahejie Formation (Table 4), the prediction results were compared with the actual in situ drilling results, considering factors such as weak-surface effects and changes in inclination and azimuth angles, as shown in Figure 10.

Table 4. In situ downhole complexity and engineering information

Well No.	Sounding/ vertical depth, m	Lithology	Density, g/cm^3	Well deviation,°	Azimuth,°	Downhole complexity
CX682	3148/2642.22	Mudstone/ sandstone interbedded	1.20	75.43	SE179.15	After hitting the ruler, the pump is held when the eye is lowered, and the jam drilling becomes complicated
LX891	3894/2963.81	Mudstone/ fine sand	1.55	41	NE72.9	Drilling fluid density: 1.34 g/cm^3, with thin flake drop (2 × 3 cm) observed

According to the prediction results, when the azimuth angle of the wellbore for Well CX682 is 179.5°, the area with high collapse pressure equivalent density is large, exhibiting the shape of a “cat’s ear.” The drilling fluid density in the field is 1.2 g/cm^3, while the predicted critical collapse pressure equivalent density is 1.56 g/cm^3. In contrast, when the azimuth of the borehole for Well LX891 is 72.9°, the area with high collapse pressure equivalent density is small, with a drilling fluid density of 1.55 g/cm^3 and a predicted critical collapse pressure equivalent density of 1.71 g/cm^3. During the drilling of both complex wells, the density of drilling fluid used was lower than the predicted critical collapse pressure equivalent density, resulting in an underbalanced drilling state. To reduce the risk of borehole collapse, the drilling fluid density should be optimized to be closer to the predicted critical collapse pressure equivalent density. At the same time, measures to inhibit formation hydration and improve the plugging ability of the drilling fluid should be implemented to further enhance wellbore stability.

By comprehensively applying the above measures, it is possible to optimize drilling fluid properties and improve wellbore stability without significantly increasing drilling fluid density, thereby reducing the risk of collapse. In actual drilling operations, these measures should be reasonably selected and combined based on the specific formation conditions and downhole situations. Additionally, real-time monitoring of downhole parameters and timely adjustments to drilling fluid properties and drilling parameters are essential to ensure a safe and efficient drilling process.

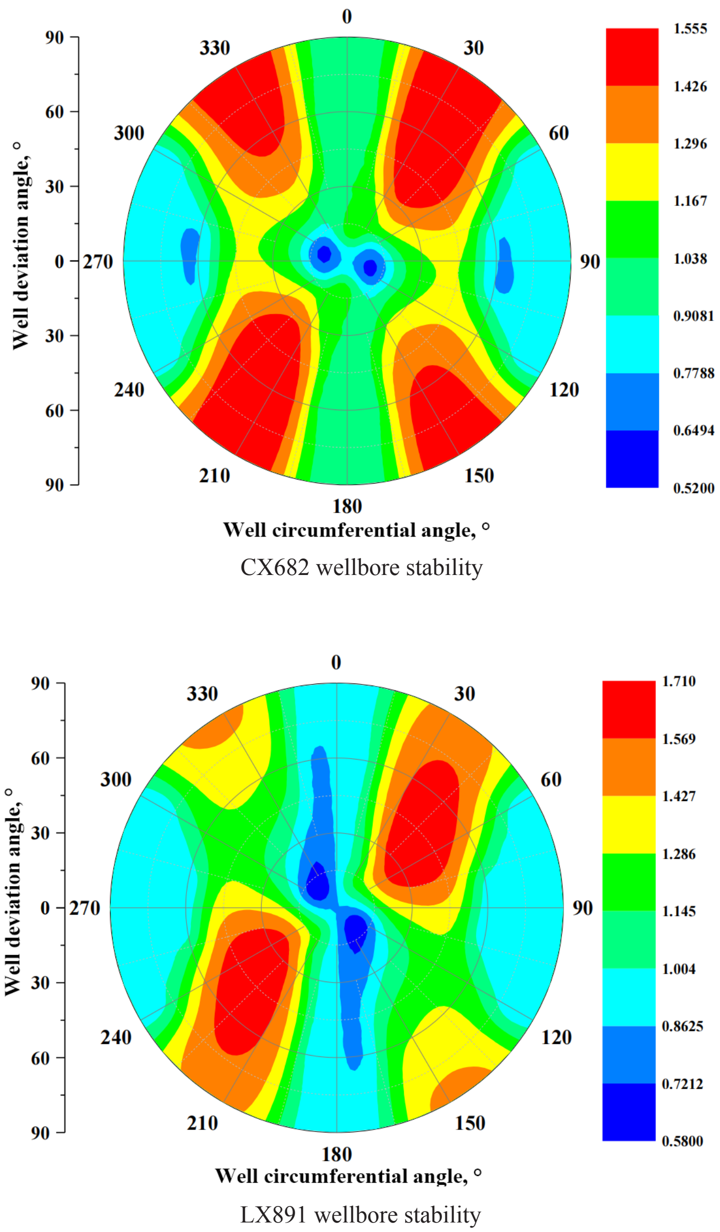

Fig. 10. Prediction of wellbore stability for two complex wells.

4. Conclusions

1. The oil shale of the Shahejie Formation has stratified bedding fractures, with a generally low fracture inclination. Local strata contain complex fracture networks, leading to high fracture connectivity and rock mass fracturing. The mineral composition of oil shale is mainly quartz and clay minerals, with the clay minerals being non-expansive and exhibiting weak hydration expansion.
2. The stability of boreholes in oil shale formations is influenced by several factors, including drilling direction, the mechanical weak surface effect of fractures, and the seepage effect of drilling fluid. Among these, the mechanical weak surface effect of fractures has the greatest impact, increasing formation collapse pressure by about 0.55 g/cm^3.
3. Wellbore stability varies significantly depending on the drilling direction. The collapse range of the borehole wall drilled along the maximum horizontal principal stress is small, with high collapse density mainly concentrated in low well-inclined sections. In contrast, the collapse range of the borehole wall drilled along the minimum horizontal principal stress is large, with high collapse density mainly concentrated in inclined and horizontal sections. In general, drilling along the maximum horizontal principal stress results in better wellbore stability than drilling along the minimum horizontal principal stress. Additionally, the seepage of drilling fluid increases the formation's equivalent density by about 0.135g/cm^3 on average. Therefore, proper plugging of the drilling fluid should be considered to improve wellbore stability in oil shale formations.

Author contribution

Shuang Du was responsible for the main writing of the paper, the design of experiments, data calculation, and field research, ensuring the integration of theory and practice. Houbin Liu provided experimental protocols and equipment, revised theoretical models, and contributed to the overall article structure. Shuai Wang assisted in experimental design and data processing, as well as correcting figures and tables to ensure data accuracy. Shuai Cui provided on-site materials, assisted in writing , reviewed key content, and contributed to the article's innovation. Jingyang Xi assisted in conceptualizing the study, rigorously reviewed data accuracy and theoretical innovation, provide field data, and verified the consistency between theoretical analysis and field applications.

Data availability statement

Data are contained within the article.

Acknowledgments

This study was financially supported by the National Natural Science Foundation of China (grant No. 52474008) and the Sichuan Provincial Natural Science Foundation (grant No. 24NSFSC2397). The authors sincerely thank all reviewers for their abundant critical and constructive comments. The publication costs of this article were partially covered by the Estonian Academy of Sciences.

References

1. Shi, B., Hu, X., Gao, S., Xu, J., Lin, Y. Visualization sealing simulation test and evaluation of hard brittle shale microfracture. *Pet. Drill. Tech.*, 2014, **42**(3), 32–37.
2. Wang, P., Qu, Z., Huang, H. Experimental study of the effect of formation water salinity on creep laws of the hard brittle shale. *Pet. Drill. Tech.*, 2015, **43**(5), 63–68. https://dx.doi.org/10.11911/syztjs.201505011
3. Westergaard, H. M. Plastic state of stress around a deep well. *J. Boston Soc. Civ. Eng.*, 1939, **6**(2), 107–114.
4. Hubbert, M. K., Willis, D. G. Mechanics of hydraulic fracturing. *Pet. Trans. AIME*, 1957, **210**(1), 153–168. https://doi.org/10.2118/686-G
5. Okland, D., Cook, J. M. Bedding-related borehole instability in high-angle wells. In: *SPE/ISRM Rock Mechanics in Petroleum Engineering*, July 8–10, 1998, Trondheim, SPE-47285-MS. https://doi.org/10.2118/47285-MS
6. Gupta, D., Zaman, M. Stability of boreholes in a geologic medium including the effects of anisotropy. *Appl. Math. Mech.*, 1999, **20**, 837–866. https://doi.org/10.1007/BF02452483
7. Chenevert, M. E., Gatlin, C. Mechanical anisotropies of laminated sedimentary rocks. Soc. *Pet. Eng. J.*, 1965, **5**(1), 67–77. https://doi.org/10.2118/890-PA
8. Ong, S. H., Roegiers, J.-C. Influence of anisotropies in borehole stability. *Int. J. Rock Mech. Min. Sci. Geomech. Abstr.*, 1993, **30**(7), 1069–1075. https://doi.org/10.1016/0148-9062(93)90073-M
9. Chen, X., Yang, Q., Qiu, K. B., Feng, J. L. An anisotropic strength criterion for jointed rock masses and its application in wellbore stability analyses. *Int. J. Numer. Anal. Methods Geomech.*, 2008, **32**(6), 607–631. https://doi.org/10.1002/nag.638
10. Jin, Y., Yuan, J., Hou, B., Chen, M., Lu, Y., Li, S., Zou, Z. Analysis of the vertical borehole stability in anisotropic rock formations. *J. Pet. Explor. Prod. Technol.*, 2012, **2**(4), 197–207. http://dx.doi.org/10.1007/s13202-012-0033-y
11. Paslay, P. R., Cheatham, Jr. J. B. Rock stresses induced by flow of fluids into boreholes. *Soc. Pet. Eng. J.*, 1963, **3**(1), 85–94. https://doi.org/10.2118/482-PA
12. Chen, X., Tan, C. P., Detournay, C. A study on wellbore stability in fractured rock masses with impact of mud infiltration. *J. Pet. Sci. Eng.*, 2003, **38**(3–4), 145–154. https://doi.org/10.1016/S0920-4105(03)00028-7

13. McLean, M. R., Addis, M. A. Wellbore stability analysis: a review of current methods of analysis and their field application. In: *IADC/SPE Drilling Conference*, February 27 – March 2, 1990, Houston, Texas, SPE-19941-MS. https://doi.org/10.2118/19941-MS
14. Dusseault, M. B., Gray, K. E. Mechanisms of stress-induced wellbore damage. In: *SPE Formation Damage Control Symposium*, February 26–27, 1992, Lafayette, Louisiana, SPE-23825-MS. https://doi.org/10.2118/23825-MS
15. Zhu, K., Chen, J., Lu, S. Study on stability mechanism of brittle shale borehole deep in Nanpu-III structure and its application. *Drill. Prod. Technol.*, 2016, **39**, 1–4, 100.
16. Liang, L., Ding, Y., Liu, X., Xu, L. Seepage–mechanochemistry coupling of wellbore stability in hard-brittle shale. *Spec. Oil Gas Reserv.*, 2016, **23**, 140–143, 158.
17. Qian, Z., Wu, J., Li, J., Hong, W., Ma, J., Kuang, X. Application of the oil-based drilling fluid in oil shale formation. *Pet. Geol. Oilfield Dev. Daqing*, 2016, **35**, 170–174.
18. Liu, K., Liu, S., Wen, M. Analyze of borehole wall stability by the action of physical chemistry. *Petrochem. Ind. Technol.*, 2019, **26**, 139–140.
19. Chen, Z., Deng, J., Wei, B., Hu, J. Borehole stability analysis of hard brittle shale based on damage theory. *Sci. Technol. Eng.*, 2019, **19**(16), 87–94.
20. Zhao, G., Chen, C., Yan, H., Hao, Y. Study on the damage characteristics and damage model of organic rock oil shale under the temperature effect. *Arab. J. Geosci.*, 2021, **14**(8), 722. http://dx.doi.org/10.1007/s12517-021-07046-x
21. Zhao, J., Kang, Z. Permeability of oil shale under in situ conditions: Fushun oil shale (China) experimental case study. *Nat. Resour. Res.*, 2021, **30**(12), 753–763. http://dx.doi.org/10.1007/s11053-020-09717-0
22. Zhang, R., Chen, F., Niu, H., Gao, D., Liu, X. L., Yang, C. X. Study on the collapse pressure of hard and brittle fractured oil shale in ZH sag. *Oil Drill. Prod. Technol.*, 2021, **43**(2), 151–159.
23. Ren, S., Wang, L., Yang, D., Kang, Z., Zhang, P. Effect of real-time temperature and shear angle on the mechanical strength and energy evolution of oil shale. *Oil Shale*, 2022, **39**(4), 270–289. http://dx.doi.org/10.3176/oil.2022.4.03
24. Wang, L., Yang, D., Kang, Z., Zhao, J., Meng, Q. Experimental study on the effects of steam temperature on the pore–fracture evolution of oil shale exposed to the convection heating. *J. Anal. Appl. Pyrolysis*, 2022, **164**, 105533. https://doi.org/10.1016/j.jaap.2022.105533
25. Feng, Z., Shi, J. Research on the evolution rules and mechanisms of permeability of organic rocks under the action of thermal-mechanical coupling. *J. Coal Sci. Eng. (China)*, 2023, 1–13. http://dx.doi.org/10.13225/j.cnki.jccs.2023.1296
26. Zhang, X., Yu, L., Ma, Z., Li, Y., Jiang, X. Analysis of anisotropic heat transfer properties of oil shale and simulation of in-situ thermal conduction exploitation. *J. Taiyuan Univ. Technol.*, 2024, **55**(2), 260–266. https://doi.org/10.16355/j.tyut.1007-9432.20230683

27. Cao, J., Yang, D., Kang, Z., Feng, L. Study on shear failure characteristics of oil shale under high-temperature steam treatment. *J. Taiyuan Univ. Technol.*, 2023, **55**(2), 252–259. https://doi.org/10.16355/j.tyut.1007-9432.20230637
28. Chen, M., Jin, Y., Zhang, G. *Petroleum Engineering Rock Mechanics*. Science Press, Beijing, 2008.
29. Jaeger, J. C. Shear failure of anisotropic rocks. *Geol. Mag.*, 1960, **97**(1), 65–72. https://doi.org/10.1017/S0016756800061100
30. Ma, T., Chen, P., Wang, X., Guo, Z., Liu, Z. Numerical analysis method of pore pressure propagation around the borehole for shale gas reservoirs. *Acta Petrol. Sin.*, 2016, **37**(5), 660–671. https://dx.doi.org/10.7623/syxb201605010
31. Jin, Y., Chen, M. *Wellbore Stabilization Mechanics*. Science Press, Beijing, 2012.